

RESEARCH ARTICLE

Open Access



# Time difference between the 1854 CE Ansei–Tokai and Ansei–Nankai earthquakes estimated from distant tsunami waveforms on the west coast of North America

Satoshi Kusumoto<sup>\*</sup> , Kentaro Imai and Takane Hori

## Abstract

We estimated the time difference between the 1854 CE Ansei–Tokai and Ansei–Nankai earthquakes from tidal records of two tide gauge stations (San Francisco and San Diego) on the west coast of North America. The first signals of the Ansei–Tokai tsunami were apparent, whereas those of the Ansei–Nankai tsunami were obscured by the later waves of the Ansei–Tokai tsunami. Waveforms of the Ansei–Nankai tsunami simulated with nonlinear dispersive wave theory by assuming an origin time of 07:00 GMT on 24 December arrived earlier than in the observations. The normalized root mean square and the misfit between the simulated and observed waveforms of the Ansei–Nankai tsunami showed a time difference between them of approximately 0.4 h. This finding suggests that the actual origin time of the Ansei–Nankai tsunami was approximately 07:24 GMT on 24 December. A previous study estimated the origin time of the Ansei–Tokai tsunami to be about 00:30 GMT on 23 December. Thus, we concluded that the time difference between the 1854 CE Ansei–Tokai and Ansei–Nankai tsunamis was 30.9 h. Despite the significant difference in the time resolution between the seasonal timekeeping system used in Japan in 1854 and waveform digitization, our result is roughly in agreement with historical descriptions of the tsunamis, suggesting that such information can be effectively used to determine the origin times of historical earthquakes.

**Keywords:** Historical earthquakes, Historical tsunamis, 1854 CE Ansei–Nankai tsunami, Time difference between Ansei–Tokai and Ansei–Nankai earthquakes, Historical materials, Numerical simulation of trans-Pacific tsunami

## 1 Introduction

The Nankai Trough subduction zone has repeatedly generated large earthquakes accompanied by tsunamis (e.g., Ando 1975; Ishibashi 2004). The fault region has been divided into six segments (e.g., Garrett et al. 2016; Fujiwara et al. 2020), and two main rupture patterns are observed: in the first, all segments rupture

simultaneously, whereas in the second, different segments rupture at different times, with a time lag between ruptures of a few ten hours to years. The 1707 Common Era (CE) Hoei Nankai earthquake is an example of the first pattern, whereas the 1854 CE Ansei–Tokai and Ansei–Nankai earthquakes and the 1944 CE Showa–Tonankai and 1946 CE Showa–Nankai earthquakes are examples of the second pattern. The 1944 CE and 1946 CE events occurred about two years apart (e.g., Imai et al. 2006) and the two 1854 events approximately 30–32 h apart (e.g., Usami 2003; Central Disaster Management Council 2005; Matsu'ura 2017). Thus, Nankai Trough megathrust earthquakes exhibit diverse behaviors.

\*Correspondence: kusumotos@jamstec.go.jp  
Research Institute for Marine Geodynamics, Research and Development Center for Earthquake and Tsunami Forecasting, Japan Agency for Marine–Earth Science and Technology, 3173–25 Showa-machi, Kanazawa, Yokohama 236-0001, Japan

The estimated moment magnitude of the 1854 Ansei–Tokai earthquake was  $M_w$  8.4–8.6, and that of the Ansei–Nankai earthquake was  $M_w$  8.5–8.7 (e.g., Cabinet Office Committee for Modeling a Nankai Trough Megaquake 2015; Building Research Institute 2019). Furthermore, both of these earthquakes generated huge tsunamis. In this study, we focused on the time difference between the 1854 CE Ansei–Tokai and Ansei–Nankai earthquakes. In 1854, a seasonal time system was used in Japan; the day and night were separately divided into equal parts and the length of each time unit changed seasonally along with the changing sunrise and sunset times. As a result, reported origin times for these earthquakes may not be accurate. In contrast, the signals of the tsunamis generated by these earthquakes were recorded by tide stations on the west coast of North America using the fixed time system in which each day is divided into 24 h of equal length (e.g., Bache 1856; Satake et al. 2020). Although there are several problems with the observed tsunami waveforms (e.g., the hydraulic filter at the time of observation is unknown), by comparing them with calculated waveforms, they can be used to quantitatively evaluate the tsunami origin time and time difference. In fact, Kusumoto et al. (2020) estimated the origin time of the 1854 CE Ansei–Tokai tsunami to be 00:30 on 23 December by comparing the tsunami waveforms observed at stations on the west coast of North America with calculated waveforms. In this study, we first estimated the origin time of the 1854 CE Ansei–Nankai tsunami by comparing observed and simulated waveforms. Then, we calculated the time difference between the 1854 CE Ansei–Tokai and Ansei–Nankai earthquakes by using our estimated origin time for the Ansei–Nankai tsunami and the origin time estimated by Kusumoto et al. (2020) for the Ansei–Tokai tsunami and compared the result with historical descriptions of the two earthquakes and tsunamis.

## 2 Observations of the 1854 CE Ansei–Tokai and Ansei–Nankai earthquakes

### 2.1 Historical materials

The 1854 CE Ansei–Tokai and Ansei–Nankai earthquakes and tsunamis are summarized in new collection of historical materials on earthquakes in Japan (Earthquake Research Institute of the University of Tokyo 1987, 1989a, 1989b, 1994). This is a catalog containing historical documents with many descriptions of these events. All materials for the Ansei–Tokai and Ansei–Nankai earthquakes use the seasonal timekeeping system in use at the time, and it is very difficult to convert descriptions from different prefectures using that timekeeping system to the local time system because sunrise and sunset times differed depending on location. Therefore, we focused on

historical materials from Wakayama Prefecture Japan, which is the regional boundary between the Ansei–Tokai and Ansei–Nankai earthquake epicenters (e.g., Usami 2008, 2012).

“Kotoki,” a report written in Japanese by Mr. Heibei Iwateya, a Japanese lacquerware worker who lived in Fukagawa–Kuroe city (Kuroe city at the time of the earthquakes) in the western part of the prefecture, is one of the contemporary documents for the Ansei–Tokai and Ansei–Nankai earthquakes (Yanagikawa 1977). According to this report, strong shaking occurred at eight o'clock local time on 23 December and again at seventeen o'clock local time the next day. Mr. Heibei Iwateya did not report the Ansei–Tokai tsunami, but the Ansei–Nankai tsunami caused serious damage on 24 December. This tsunami arrived at eighteen o'clock after the earthquake and repeated waves struck Kuroe city, with the third wave being the largest. On the basis of this description, the time difference between the Ansei–Tokai and Ansei–Nankai earthquakes can be estimated as approximately 32 h.

Another contemporary description is “Knowledge for Large Earthquake and Tsunami,” an inscription on a monument erected in 1856 CE by Saint Zenchō (Syoku), a priest of the Jinsen Temple who lived in Yuasa city in the western part of the prefecture (e.g., Hatori 1980; Ishibashi et al. 2017). According to this monument, large earthquakes occurred at ten o'clock local time on 23 December and at sixteen o'clock local time on 24 December. A sudden rise and fall of the tide occurred on 23 December that caused no damage, but on 24 December, a large tsunami destroyed houses, ships, and warehouses and caused catastrophic damage to the entire settlement. On the basis of this description, the time difference between the Ansei–Tokai and Ansei–Nankai earthquakes can be inferred to be about 30 h.

The “Diary of Koza Kirimeya,” written in Japanese by the Kirimeya owner, who lived in Koza city in the southern part of the prefecture, is also the contemporary document for the Ansei–Tokai and Ansei–Nankai earthquakes (e.g., Hamahata 1977; Imai et al. 2017). According to this diary, strong shaking occurred at ten o'clock on 23 December and sixteen o'clock on 24 December. The Ansei–Tokai tsunami arrived immediately, but was not high. The Ansei–Nankai tsunami repeatedly struck, and the second wave was the highest. On the basis of this account, the time difference between the Ansei–Tokai and Ansei–Nankai earthquakes can again be estimated to be approximately 30 h.

### 2.2 Instrumental observations

In 1853, tide gauge stations were installed at three sites on the west coast of the USA: Astoria, Oregon, and San

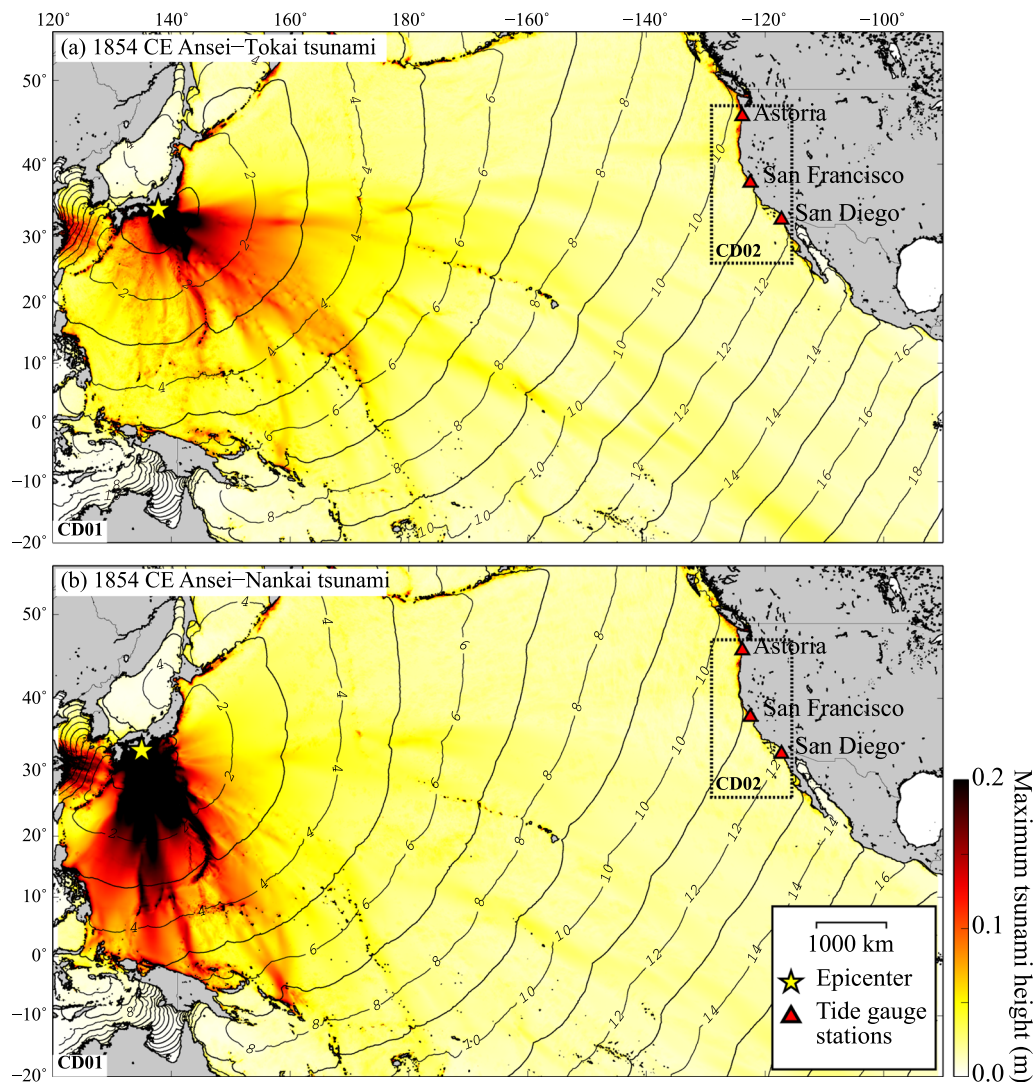


**Fig. 1** Distributions of maximum tsunami heights and tsunami travel times of the 1854 CE **a** Ansei-Tokai and **b** Ansei-Nankai earthquakes. CD01 and CD02 are the computational domains of 54 and 18 s in grid intervals, respectively. The contour interval is 1 h. The earthquake epicenters are shown by yellow stars, and the locations of the North American tide gauge stations are shown by red squares

San Francisco and San Diego, California (Figs. 1, 2). These stations used a mechanical clock to record accurate times of high and low tides (U. S. Coast Survey 1855). Between 23 and 25 December 1854 CE, rapid rises and falls of seawater were observed at these tide gauge stations (Bache 1856). Two years later, these abnormal seawater rises and falls were recognized as the 1854 CE Ansei-Tokai and Ansei-Nankai tsunamis, after they had traversed the Pacific Ocean (e.g., Honda et al. 1908; Omori 1913).

In this study, we used only the tsunami signals recorded at the tide gauge stations in San Francisco and San Diego because the tsunami signal observed at the Astoria tide gauge station was considered too ambiguous to use. The

high noise level was possibly caused by storm surges or the tsunami; a sketch of the Pacific Northwest coast about 55 km north of Astoria published in 1857 shows flooding that occurred between 23 and 25 December (Cooper 1853–1854; Tolkova et al. 2015).

### 3 Numerical analysis

Numerical simulation of trans-Pacific tsunami propagation was performed by using the staggered leap-frog scheme in the JAGURS tsunami simulation code (e.g., Baba et al. 2017). Trans-Pacific tsunami propagation was calculated on the basis of two-dimensional nonlinear dispersive wave theory with Coriolis force and Boussinesq

**Table 1** Fault parameters of the 1854 CE Ansei-Tokai and Ansei-Nankai earthquakes (An'naka et al. 2003)

Subfault no.	Length (km)	Width (km)	Depth (km)	Strike (deg)	Dip (deg)	Rake (deg)	Slip (m)	Latitude (deg N)	Longitude (deg E)
Ansei-Tokai earthquake									
N1	120	50	6.4	193	20	71	5.27	35.120	138.706
N2	205	100	4.1	246	10	113	5.50	33.823	138.235
Ansei-Nankai earthquake									
N3	155	100	7.8	251	12	113	4.80	33.006	136.074
N4	125	120	10.1	250	8	113	8.70	32.614	134.481

terms in a spheroidal coordinate system. The governing equations are expressed as follows:

$$\begin{aligned} \frac{\partial M}{\partial t} + \frac{1}{R \sin \theta} \frac{\partial}{\partial \varphi} \left( \frac{M^2}{H + \eta} \right) + \frac{1}{R} \frac{\partial}{\partial \theta} \left( \frac{MN}{H + \eta} \right) \\ = -\frac{g(H + \eta)}{R \sin \theta} \frac{\partial \eta}{\partial \varphi} - fN - \frac{gn^2}{(H + \eta)^{7/3}} M \sqrt{M^2 + N^2} \\ + \frac{H^2}{3R \sin \theta} \frac{\partial}{\partial \varphi} \left[ \frac{1}{R \sin \theta} \left( \frac{\partial^2 M}{\partial \varphi \partial t} + \frac{\partial^2 (N \sin \theta)}{\partial \theta \partial t} \right) \right] \end{aligned} \quad (1)$$

$$\begin{aligned} \frac{\partial N}{\partial t} + \frac{1}{R \sin \theta} \frac{\partial}{\partial \varphi} \left( \frac{MN}{H + \eta} \right) + \frac{1}{R} \frac{\partial}{\partial \theta} \left( \frac{N^2}{H + \eta} \right) \\ = -\frac{g(H + \eta)}{R} \frac{\partial \eta}{\partial \theta} + fM - \frac{gn^2}{(H + \eta)^{7/3}} N \sqrt{M^2 + N^2} \\ + \frac{H^2}{3R} \frac{\partial}{\partial \theta} \left[ \frac{1}{R \sin \theta} \left( \frac{\partial^2 M}{\partial \varphi \partial t} + \frac{\partial^2 (N \sin \theta)}{\partial \theta \partial t} \right) \right] \end{aligned} \quad (2)$$

where  $M$  and  $N$  are the discharge fluxes in the longitudinal ( $\varphi$ ) and co-latitudinal ( $\theta$ ) directions, respectively,  $H$  is the water depth of the ocean,  $\eta$  is the wave amplitude,  $g$  is the gravity ( $9.81 \text{ m/s}^2$ ),  $t$  is the time,  $R$  is the radius of the Earth ( $6371 \text{ km}$ ),  $f$  is the Coriolis parameter ( $2\Omega \sin \theta$ ; here,  $\Omega$  is the angular frequency of the Earth rotation ( $7.27 \times 10^{-5} \text{ rad/s}$ )), and  $n$  is the Manning's roughness coefficient ( $0.025 \text{ s m}^{-1/3}$ ). The volume change per unit time must be equal to the flow rate of water into the volume. Therefore, the continuity equation is:

$$\frac{\partial \eta}{\partial t} = -\frac{1}{R \sin \theta} \left[ \frac{\partial M}{\partial \varphi} + \frac{\partial (N \sin \theta)}{\partial \theta} \right]. \quad (3)$$

Trans-Pacific tsunamis exhibit a phase delay owing to the elasticity of the Earth and the vertical compressibility of seawater (e.g., Allgeyer and Cummins 2014; Watada et al. 2014). Therefore, we applied the Green's function that describes the response to a unit mass load concentrated at a point on the surface as proposed by Allgeyer and Cummins (2014), which can be expressed as:

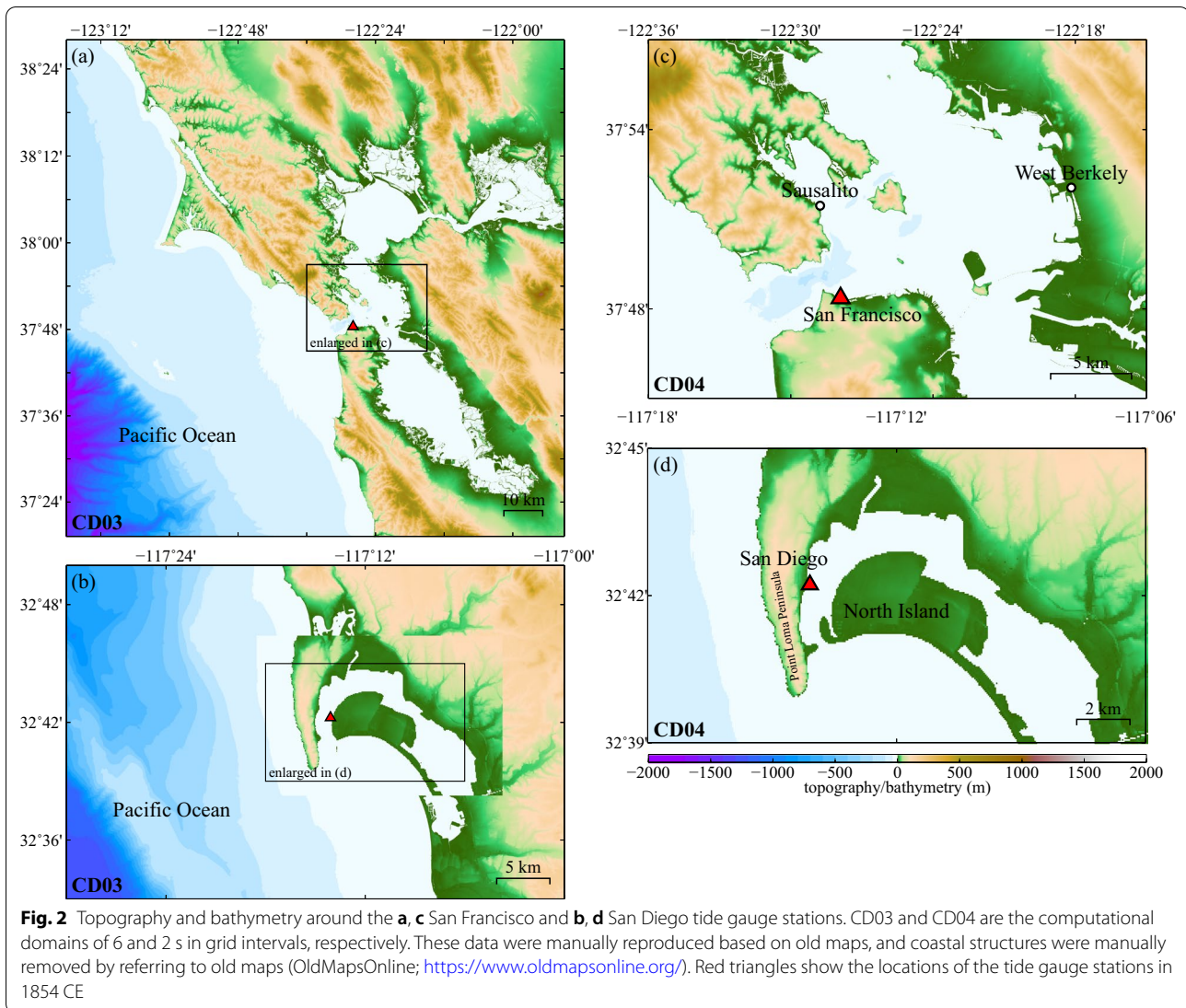
$$G(\mathbf{r}', \mathbf{r}) = \frac{R}{M_e} \sum_{n=0}^{\infty} h'_n P_n(\cos \alpha) \quad (4)$$

where  $\mathbf{r}$  denotes a position on the Earth's surface with the point mass located at  $\mathbf{r}'$ ,  $P_n$  refers to the  $n$ th Legendre polynomial,  $\alpha$  is the angular distance between  $\mathbf{r}'$  and  $\mathbf{r}$ ,  $M_e$  is the mass of the Earth, and  $h'_n$  is the loading Love number of angular order  $n$ .

The tide gauge records reported in Omori (1913) have been digitized at 1-min intervals (Fig. 3, Kusumoto et al. 2020). The effects on the observed tsunami waveform of filtering due to the structure of the water pipe at the tide gauge station at the time of the earthquake and changes in the hydraulic response are unknown, and there is no information available that allows them to be estimated. Therefore, we extracted the high-energy period band from the amplitude spectrum of the observed waveforms as follows. First, the amplitudes were normalized by the maximum amplitude in the time window covered by the simulation. Next, the bandpass filter cut-off period was determined from the amplitude spectrum of the observed waveforms. The tidal components were removed by applying a high-pass filter with a cut-off period of 128 min. Figure 3 shows the resulting amplitude spectrum. The maximum energy was observed at periods of 30–80 min, and when the period was 16 min, the energy level was approximately 1/10 of the maximum. Therefore, the cut-off period of the low-pass filter was set to 16 min. The time resolution was set to 0.1 h, which is 1/10 of the time unit of the original recording.

As the tsunami source model for the 1854 CE Ansei-Tokai and Ansei-Nankai earthquakes, we used the An'naka model, which was inferred from tsunami inundation and run-up heights (Table 1; An'naka et al. 2003). Crustal deformation, including horizontal displacement on the seafloor slope, was computed for the source model (e.g., Okada 1985; Tanioka and Satake 1996), and the Kajiura filter was applied to convert crustal displacement to initial sea surface displacement (Kajiura 1963). To numerically model the tsunami, we adopted a nested grid system in which the nested grids included 54, 18,





6, and 2 arc-seconds in the spherical coordinate system (Figs. 1, 2). To produce the nested grid system, the General Bathymetric Chart of the Oceans ([https://www.gebco.net/data\\_and\\_products/gridded\\_bathymetry\\_data/gebco\\_2021/](https://www.gebco.net/data_and_products/gridded_bathymetry_data/gebco_2021/)) and high-resolution (1/3 arc-second) coastal digital elevation and depth models from the U.S. National Oceanic and Atmospheric Administration were combined and resampled. Coastal structures constructed after 1854 CE were manually removed by referring to old topographic maps. A time step of 0.5 s was used in our simulations to ensure computational stability of the finite-difference algorithm with the finest grid.

The first signal of the Ansei–Nankai tsunami was obscured by later waves of the Ansei–Tokai tsunami. Therefore, we conducted a wavelet analysis of the observed waveforms to judge the arrival time of the

Ansei–Nankai tsunami by applying Wavelet Analysis Package Software developed by Torrence and Compo (1998). We used the Morlet function with a scaling parameter as the wavelet mother function.

To compare the simulated and observed waveforms, we used the normalized root mean square (NRMS) and the NRMS misfit values calculated as follows (e.g., Heidarzadeh et al. 2016):

$$\text{NRMS}_k = \frac{\sqrt{\sum_{i=1}^N (\text{obs}_i - \text{sim}_i)^2}}{\sqrt{\sum_{i=1}^N (\text{obs}_i - \overline{\text{obs}})^2}} \quad (5)$$

$$\text{NRMS misfit} = \frac{\sum_{k=1}^M \text{NRMS}_k}{M} \quad (6)$$

where  $NRMS_k$  is the NRMS for San Francisco or San Diego,  $N$  is the number of sampled records at the station,  $obs_i$  and  $sim_i$  are observed and simulated waveforms, respectively, and  $\overline{obs}$  is the average of the observed waveform at each station.  $M$  is the number of stations; thus,  $M=2$  (i.e., San Francisco and San Diego). The simulations are consistent with the observations if the indicator values are close to zero.

## 4 Results and discussion

### 4.1 Characteristics of the tsunami signals

The observed and simulated waveforms at the San Francisco and San Diego tide gauge stations are compared in Fig. 4. The first signals of the 1854 CE Ansei-Tokai tsunami were apparent, whereas those of the 1854 CE Ansei-Nankai earthquake were obscured by later waves of the Ansei-Tokai tsunami. Comparing the initial observed waveforms of the Ansei-Tokai and Ansei-Nankai tsunamis at each tide station, the wavelength of the Ansei-Nankai tsunami was relatively longer than that of the Ansei-Tokai tsunami. This characteristic was reproduced by the numerical simulation. Near San Francisco and San Diego, the longer wavelength of the Ansei-Nankai tsunami, which was generated in the direction parallel to the trench axis, relative to that of the Ansei-Tokai

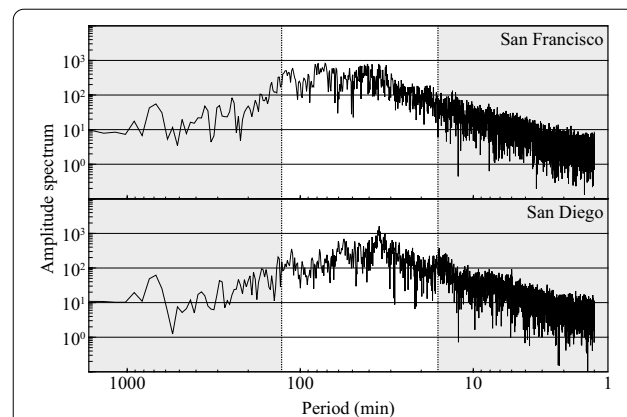


**Fig. 3** Amplitude spectra for the observed waveforms including the both Ansei-Tokai and Ansei-Nankai tsunami events (from 3 am 23 December until 7 am 26 December) at the San Francisco and San Diego tide gauge stations. Portions of the energy band removed by application of the low- and high-bandpass filters (cut-off periods of 16 and 128 min, respectively) are shaded gray

tsunami, which was generated in the direction orthogonal to the trench axis, probably reflects the relationship between the direction of the fault strike and the orientation of the west coast of North America (Figs. 1, 4).

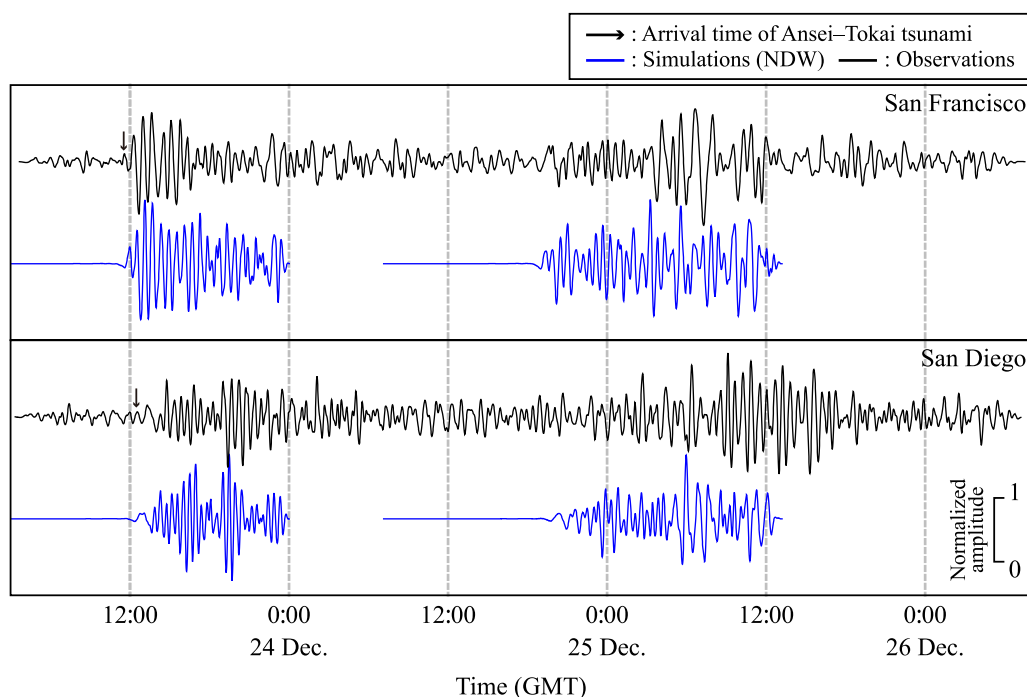


**Fig. 4** Comparison of observations and nonlinear dispersive wave (NDW) simulation results for the San Francisco and San Diego tide gauge stations. Black and blue curves show the observed and simulated waveforms, respectively, after application of low- and high-bandpass filters with cut-off periods of 16 and 128 min, respectively

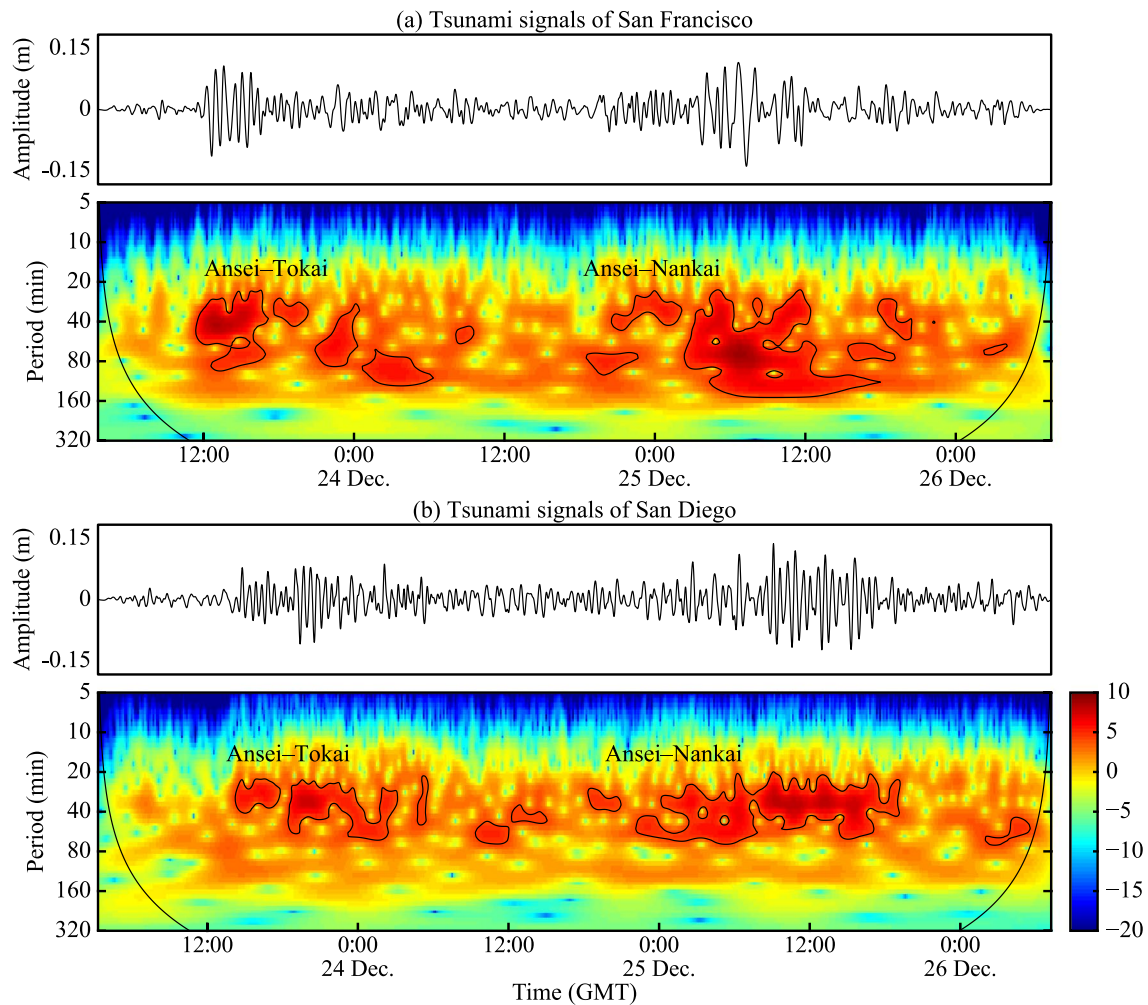


**Fig. 5** Wavelet analysis results for the tsunami signals recorded at the **a** San Francisco and **b** San Diego tide gauge stations. The amplitudes have not been normalized. Contour lines show the 95% confidence interval

Here, we applied wavelet analysis to study temporal variations of tsunami dominant periods (e.g., Heidarzadeh et al. 2021). The Ansei–Tokai tsunami was characterized by dispersive waves that subsequently became protracted, whereas the Ansei–Nankai tsunami was characterized initially by small wave packets and subsequently by large-amplitude, high-energy waves (Fig. 5). At the San Francisco tide gauge station, the periods of the later waves were dominantly 25–100 min for the Ansei–Tokai tsunami and 25–133 min for the Ansei–Nankai tsunami. The dominant period of the Ansei–Nankai tsunami waves roughly matches the fundamental oscillation (period about 116 min) between the Sausalito and West Berkeley sides of San Francisco Bay for waves incident on the Golden Gate (Honda et al. 1908). Therefore, the later waves of the Ansei–Nankai tsunami may correspond to the oscillations in

San Francisco Bay. In contrast, at the San Diego tide gauge station, the dominant period had an upper limit of about 70 min.

#### 4.2 Origin times of the 1854 CE Ansei–Nankai tsunamis

The simulated tsunami waves reached the west coast of North America about 11–12 h after the earthquake (Fig. 1). When the observed waveforms were compared with those simulated by assuming that the 1854 CE Ansei–Nankai tsunami originated at 07:00 GMT on 24 December, the observed waveforms lagged behind the simulated waveforms by several tens of minutes (Fig. 7). Figure 6 shows the NRMS and the NRMS misfit between the simulated waveforms and those observed at the San Francisco and San Diego tide gauge stations. The minimum NRMS misfit value

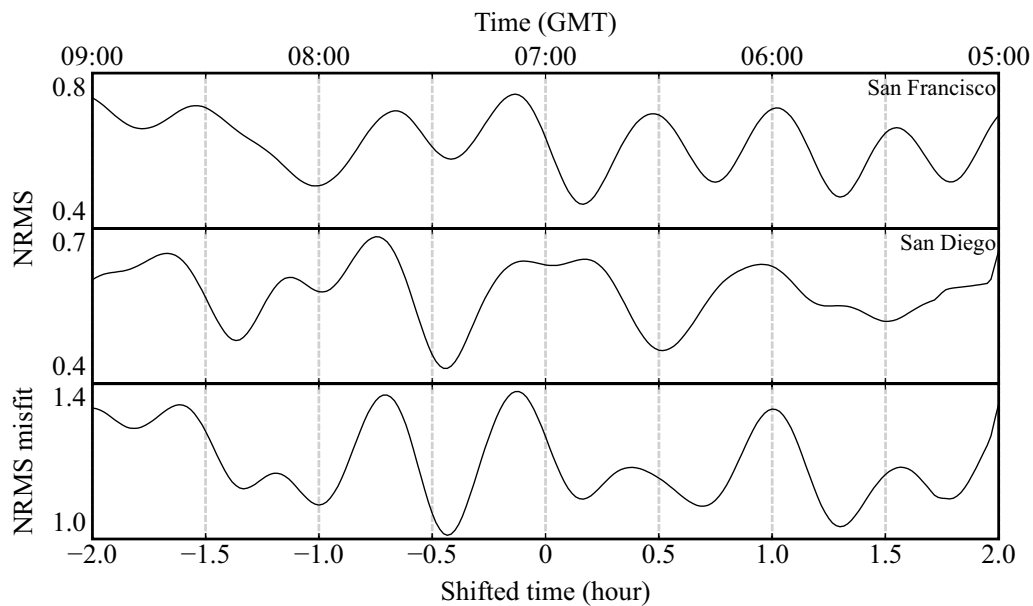


**Fig. 6** Normalized root mean square (NRMS) and NRMS misfit between observed and simulated waveforms of the 1854 CE Ansei–Nankai tsunami at the San Francisco and San Diego tide gauge stations

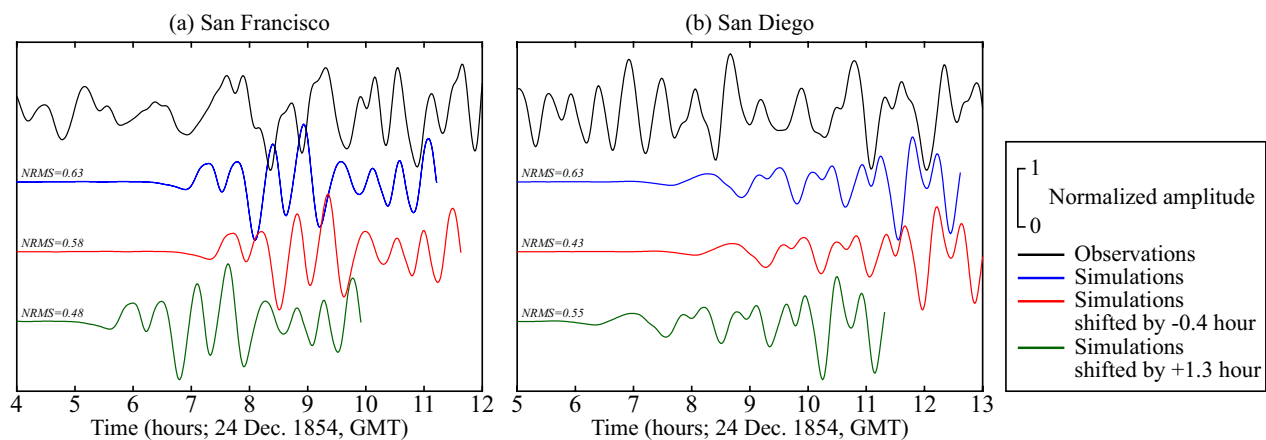


**Fig. 7** Comparison of observed and simulated waveforms of the 1854 CE Ansei–Nankai tsunami recorded at the **a** San Francisco and **b** San Diego tide gauge stations. Black, blue, red, and green curves show the observations, simulations, and simulations shifted by  $-0.4$  h and  $+1.3$  h, respectively

was calculated when the simulated waveforms were shifted by  $-0.4$  h or  $+1.3$  h. However, the NRMS value between observation and simulation shifted by  $+1.3$  h at the tide gauge station of San Diego was not a minimum (Figs. 6, 7). Conversely, the NRMS values between observed and simulated waveforms shifted by  $-0.4$  h at the tide gauge stations of San Francisco and San Diego had a common negative peak (Fig. 6). Therefore, we estimated the origin time of the 1854 Ansei–Nankai tsunami to be 07:24 GMT on 24 December (Fig. 7).

#### 4.3 Time difference between the Ansei–Tokai and Ansei–Nankai earthquakes

Kusumoto et al. (2020) compared simulated and observed waveforms recorded at San Francisco and San Diego tide gauge stations and concluded that the origin time of the 1854 CE Ansei–Tokai tsunami was 00:30 GMT on 23 December. Similarly, we estimated the origin time of the 1854 Ansei–Nankai tsunami to be 07:24 GMT on 24 December. Thus, we can estimate the time difference between these earthquakes to be approximately 30.9 h.



#### 4.4 Comparison with descriptions in historical documents

According to historical descriptions in Wakayama Prefecture documents, the 1854 CE Ansei–Nankai earthquake occurred at about 16:00 local time on 24 December. Local time in Wakayama Prefecture was 9 h and 1–3 min ahead of GMT. Thus, our estimated origin time of the Ansei–Nankai tsunami of 07:24 GMT is equivalent to about 16:24 local time in Wakayama Prefecture. This result is roughly consistent with the information in the historical materials.

The time difference between the 1854 CE Ansei–Tokai and Ansei–Nankai earthquakes estimated from historical materials ranges from 30 to 32 h (e.g., Usami 2003; Central Disaster Management Council 2005; Matsu'ura 2017). Thus, the resolution of the seasonal timekeeping system used in Japan at the time of the earthquakes was approximately 2 h. In contrast, the time resolution of our study was much higher at 0.1 h. Therefore, our result (30.9 h) is consistent with the time difference of about 30–32 h based on historical materials. This finding suggests that information in historical documents can be effectively used to determine the origin times of historical earthquakes if the temporal error due to the use of the seasonal timekeeping system can be tolerated.

## 5 Conclusions

We estimated the origin time of the 1854 CE Ansei–Nankai tsunami and the time difference between the Ansei–Tokai and Ansei–Nankai earthquakes from tidal records of the San Francisco and San Diego tide gauge stations in North America. By comparing the observations with simulations in which it was assumed that the 1854 CE Ansei–Nankai tsunami originated at 07:00 GMT on 24 December, we found that the observed waveforms of the Ansei–Nankai tsunami lagged behind the simulated waveforms by 0.4 h. Therefore, we estimated the origin time of Ansei–Nankai tsunami as 07:24 GMT on 24 December. Kusumoto et al. (2020) estimated the origin time of the 1854 Ansei–Tokai tsunami to be 00:30 GMT on 23 December; thus, we estimated the time difference between the Ansei–Tokai and Ansei–Nankai tsunamis to be approximately 30.9 h. Our result is in rough agreement with descriptions in historical materials (30–32 h; e.g., Usami 2003; Central Disaster Management Council 2005; Matsu'ura 2017) if the substantial difference in temporal resolution between the seasonal timekeeping system (approximately 2 h) and the waveform digitization (0.1 h) is taken into account. This finding suggests that information in historical documents can be extremely useful for determining the origin times of historical earthquakes.

#### Abbreviations

NDW: Nonlinear dispersive wave; NRMS: Normalized root mean square; GMT: Greenwich Mean Time.

#### Acknowledgements

We would like to thank the editor (Prof. Takuto Maeda) and two anonymous reviewers for providing valuable comments and suggestions that helped to improve the manuscript. We also thank Professor Brian Atwater for providing information about the Astoria tide gauge station.

#### Authors' contributions

KI and TH contributed to the interpretation of the data. All authors read and approved the final manuscript.

#### Funding

This work was supported by the Research Project for Disaster Prevention on the great Earthquakes along the Nankai trough.

#### Availability of data and materials

The datasets supporting the conclusions of this article are available in supplementary information of Kusumoto et al. (2020) (available at <https://doi.org/10.1785/0220200068>).

#### Declarations

#### Competing interests

The authors declare that they have no competing interests.

Received: 31 August 2021 Accepted: 11 November 2021

Published online: 05 January 2022

#### References

- Allgeyer S, Cummins P (2014) Numerical tsunami simulation including elastic loading and seawater density stratification. *Geophys Res Lett* 41:2368–2375. <https://doi.org/10.1002/2014GL059348>
- Ando M (1975) Source mechanisms and tectonic significance of historical earthquakes along the Nankai Trough, Japan. *Tectonophysics* 27:119–140. [https://doi.org/10.1016/0040-1951\(75\)90102-X](https://doi.org/10.1016/0040-1951(75)90102-X)
- An'naka T, Inagaki K, Tanaka H, Yanagisawa K (2003) Characteristics of great earthquakes along the Nankai trough based on numerical tsunami simulation. *J Earthq Eng* 27:307
- Baba T, Allgeyer S, Hossen J, Cummins PR, Tsumura H, Imai K, Ymashita K, Kato T (2017) Accurate numerical simulation of the far-field tsunami caused by the 2011 Tohoku earthquake, including the effects of Boussinesq dispersion, seawater density stratification, elastic loading, and gravitational potential change. *Ocean Model* 111:46–54. <https://doi.org/10.1016/j.ocemod.2017.01.002>
- Bache AD (1856) Notice of earthquake waves on the western coast of the United States, on the 23rd and 25th of December, 1854. *Am J Sci Arts* 21:37–43
- Building Research Institute (2019) Source model and deep underground structure model for long-period ground motion evaluation, Attachment 2 Appendix 3 (in Japanese) <https://www.kenken.go.jp/japanese/contents/topics/lpe/>
- Cabinet Office Committee for Modeling a Nankai Trough Megaquake (2015) Long-period ground motion due to a huge earthquake along the Nankai Trough (in Japanese) [http://www.bousai.go.jp/jishin/nankai/nankaitrou gh\\_report.html](http://www.bousai.go.jp/jishin/nankai/nankaitrou gh_report.html)
- Central Disaster Management Council (2005) Business Continuity Guideline, Cabinet Office, Government of Japan, 19–103 (in Japanese). [http://www.bousai.go.jp/kyoiku/kyokun/kyoukunnokeshou/rep/1854\\_ansei\\_toukai\\_nankai\\_jishin/index.html](http://www.bousai.go.jp/kyoiku/kyokun/kyoukunnokeshou/rep/1854_ansei_toukai_nankai_jishin/index.html)
- Cooper JG (1853–1854) NOTE BOOK, Transcribed and Reviewed by Digital Volunteers Extracted April 08 2020.
- Earthquake Research Institute (1987) New collection of historical materials on earthquakes in Japan, vol S5-5-1&2. ERI, Tokyo, pp 2528 (in Japanese)
- Earthquake Research Institute (1989) New collection of historical materials on earthquakes in Japan, Suppl. S. ERI, Tokyo, pp 992 (in Japanese)
- Earthquake Research Institute (1994) New collection of historical materials on earthquakes in Japan, Add. Suppl. S. ERI, Tokyo, pp 1228 (in Japanese)
- Fujiwara O, Goto K, Ando R, Garrett E (2020) Paleotsunami research along the Nankai Trough and Ryukyu Trench subduction zones -current achievements and future challenges. *Earth Sci Rev* 210:103333

- Garrett E, Fujiwara O, Garrett P, Heyvaert VMA, Shishikura M, Yokoyama Y, Hubert-Ferrari A, Brückner H, Nakamura A, Batist MD (2016) A systematic review of geological evidence for Holocene earthquakes and tsunamis along the Nankai-Suruga Trough, Japan. *Earth Sci Rev* 159:337–357. <https://doi.org/10.1016/j.earscirev.2016.06.011>
- Hamahata E (1977) Continued historical materials of the Kumano city, pp 203–208
- Hatori T (1980) Field investigation of the Nankaido tsunamis in 1707 and 1854 along the Osaka and Wakayama Coasts, West Kii Peninsula. *Bull Earthq Res Inst* 55(2):505–535 **(in Japanese)**
- Heidarzadeh M, Murotani S, Satake K, Ishibe T, Gusman AR (2016) Source model of the 16 September 2015 Illapel, Chile Mw 8.4 earthquake based on teleseismic and tsunami data. *Geophys Res Lett* 43(2):643–650
- Heidarzadeh M, Pranantyo IR, Okuwaki R, Dogan GG, Yalciner AC (2021) Long tsunami oscillations following the 30 October 2020 Mw 7.0 Aegean Sea earthquake: observations and modelling. *Pure Appl Geophys*. <https://doi.org/10.1007/s00024-021-02761-8>
- Honda K, Terada T, Yoshida Y, Isitani D (1908) An investigation on the secondary undulations of oceanic tides. *J Coll Sci Imper Univ Tokyo*. <https://doi.org/10.1080/14786440809463750>
- Imai S, Kanamori Y, Shuto N (2006) Tsunami Digital Library, J. Gonzalo et al (Eds.) ECDL2006, LNCS 4172, pp. 555–558. [http://tsunami-dl.jp/old-content/TSUNAMI/TDL\\_top\\_e.html](http://tsunami-dl.jp/old-content/TSUNAMI/TDL_top_e.html)
- Imai K, Ishibashi M, Namegaya Y, Ebina Y (2017) Field survey for tsunami trace height during the 1854 Ansei Nankai tsunami along the Wakayama Coast. *Res Rep Tsunami Eng* 33:121–130 **(in Japanese)**
- Ishibashi K (2004) Status of historical seismology in Japan. *Ann Geophys* 47(2–3):339–368. <https://doi.org/10.4401/ag-3305>
- Ishibashi M, Maeda M, Imai K, Takahashi N, Baba T, Obayashi R, Inazumi T (2017) The tsunami monument distribution along the coast of Wakayama Prefecture. *Res Rep Tsunami Eng* 33:109–120
- Kajiura K (1963) The leading wave of a tsunami. *Bull Earthq Res Inst Univ Tokyo* 41:535–571
- Kusumoto S, Imai K, Obayashi R, Hori T, Takahashi N, Ho TC, Uno K, Tanioka Y, Satake K (2020) Origin time of the 1854 Ansei–Tokai tsunami estimated from tide gauge records on the west coast of North America. *Seismol Res Lett* 91(5):2624–2630. <https://doi.org/10.1785/0220200068>
- Matsuura R (2017) Earthquake forecasting and the large-scale earthquake countermeasures act. *Monogr Seismol Soc Jpn* 5:15–19 **(in Japanese)**
- Okada Y (1985) Surface displacement due to shear and tensile faults in a half-space. *Bull Seismol Soc Am* 75(4):1135–1154
- Omori F (1913) An account of the destructive earthquakes in Japan. *Publ Eq Inv Com* 68B:1–179 **(in Japanese)**
- Satake K, Heidarzadeh M, Quiroz M, Cienfuegos R (2020) History and features of trans-oceanic tsunamis and implications for Paleo-tsunami studies. *Earth Sci Rev* 202:103112. <https://doi.org/10.1016/j.earscirev.2020.103112>
- Tanioka Y, Satake K (1996) Tsunami generation by horizontal displacement of ocean bottom. *Geophys Res Lett* 23(8):861–864
- Tolkova E, Tanaka H, Roh M (2015) Tsunami observations in rivers from a perspective of tsunami interaction with tide and riverine flow. *Pure Appl Geophys* 172:953–968
- Torrence C, Compo GP (1998) A practical guide to wavelet analysis. *Bull Am Meteorol Soc* 79:61–78
- U. S. Coast Survey (1855) Annual Report of the Superintendent of the Coast Survey, National Oceanic and Atmosphere Administration, 288 pp.
- Usami T (2003) Materials for comprehensive list of Japanese destructive earthquakes [Latest Edition] [416]–2001. Univ Tokyo Press, Tokyo, p 605 **(in Japanese)**
- Usami T (2008) Addendum of historical documents on earthquakes in Japan, 4–1&2, T. Tokyo, Usami, pp. 1874 **(in Japanese)**
- Usami T (2012) Addendum of historical documents on earthquakes in Japan, 5–1&2, T. Usami, Tokyo, pp 1526 **(in Japanese)**
- Watada S, Kusumoto S, Satake K (2014) Traveltime delay and initial phase reversal of distant tsunamis coupled with the self-gravitating elastic Earth. *J Geophys Res Solid Earth*. <https://doi.org/10.1002/2013JB010841>
- Yanagikawa K (1977) The tsunamis records by Iwateya Heibei in Kuroe. *Kainan-Shishi* 3:33–37 **(in Japanese)**

## Publisher's Note

Springer Nature remains neutral with regard to jurisdictional claims in published maps and institutional affiliations.